DOI https: //doi. org/10.1007/s11595-022-2503-5

Dynamic Recrystallization Behavior of 7056 Aluminum Alloys during Hot Deformation

SHI Guohui[1], ZHANG Yong'an[1*], LI Xiwu[1], LI Zhihui[1], YAN Lizhen[1], YAN Hongwei[1], LIU Hongwei[1], XIONG Baiqing[1,2]

(1. State Key Laboratory of Nonferrous Metals and Processes, GRIMAT Engineering Institute Co., Ltd., Beijing 101407, China; 2. GRINM Group Co., Ltd., Beijing 100088, China)

Abstract: To investigate the dynamic recrystallization behavior of 7xxx aluminum alloys, the isothermal compression tests were carried on the 7056 aluminum alloy in the temperatures range of 320-440 ℃ and in the strain rates range of 0.001-1 s^{-1}. In addition, the microstructure of samples were observed via electron back scanning diffraction microscope. According to the results, true stress and true strain curves were established and an Arrhenius-type equation was established, showing the flow stress increases with the temperature decreasing and the strain rate increasing. The critical strain (ε_c) and the critical stress (σ_c) of the onset of dynamic recrystallization were identified via the strain hardening rate and constructed relationship between deformation parameters as follows: $\varepsilon_c=6.71\times10^{-4}Z^{0.137\,3}$ and $\sigma_p=1.202\sigma_c+12.691$. The DRX is incomplete in this alloy, whose volume fraction is only 20% even if the strain reaches 0.9. Through this study, the flow stress behavior and DRX behavior of 7056 aluminum alloys are deeply understood, which gives benefit to control the hot working process.

Key words: Al-Zn-Mg-Cu alloys; flow stress behavior; dynamic recrystallization; hot deformation

1 Introduction

7xxx aluminum alloys (Al-Zn-Mg-Cu alloys) are widely used in the field of aviation due to their high strength to weight ratio and well stress corrosion resistance[1,2]. To enhance the comprehensive properties of alloys, hot working is an indispensable process for manufacturing this type alloys[3]. Dynamic recovery (DRV) and dynamic recrystallization (DRX) are two modes for microstructural evolution during hot working, which decrease the resistance to deformation. Once hot deformation begins, the DRV will begin immediately, but the DRX will not begin until both the hot activation energy and the driving energy exceed the critical value[4-6]. Although Al-Zn-Mg-Cu alloys have a high stacking fault energy, many researches have verified that DRX does exist in their hot deformation process[7]. For Al-Zn-Mg-Cu alloys, the high alloying gives more particles which pin dislocations motion and bring high distortion energy, resulting in activating the DRX[8]. It is easy to understand the hot deformation parameters have effect on the DRX behavior, which in turn affects microstructure characteristics. So, understanding the relationship between deformation parameters and the DRX allows us to optimize the microstructure during deform process[9,10].

The DRX grains are easily identified by morphology via electron backed scan diffraction (EBSD), however, the critical state of the onset of DRX is hard to quantitatively analyze in experimental ways [11, 12]. Fortunately, there is a theoretical method to do this job with the flow stress behavior of alloys [13]. As well know, the flow stress has a pronounced interaction with microstructure characteristics, thus, it is realizable to study DRX behavior through the flow stress analysis. The method states the inflection point in the strain hardening rate (θ)- strain(ε) curves where the DRX begins at the given deformation condition and the strain hardening rate is equal to the increase rate of flow stress with strain. This method has been carried on many alloys, such as Al-Cu-Li alloys[14], 42CrMo steel[15], 20MnNiMo steel[16], nickel-based superalloy[17], and AZ31B magnesium alloy [13], but not on the Al-Zn-

(Received: Mar. 26, 2021; Accepted: May 18, 2021)

SHI Guohui(石国辉): Ph D; E-mail: sgh528100@163.com

*Corresponding author: ZHANG Yong'an(张永安): Prof.; Ph D; E-mail: zhangyonganskl2017@163.com

Funded by the National Key R&D Program of China (Nos. 2016YFB0300803, 2016YFB0300903) and the National Program of China (No. 2012CB619504)

Mg-Cu alloys. The flow stress behavior can be studied with constitutive models that describes the relation between flow stress and deformation conditions. In present work, the critical state of the onset of DRX of an Al-Zn-Mg-Cu alloys under various deformation conditions will be studied, and a constitutive model will be established to analyze the flow stress behavior of the alloy.

2 Experimental

The 7056 aluminum alloy is employed in the present study, and its composition is presented in Table 1.The semi-continuously cast billets were homogenized at 470 ℃ for 2 hours. Samples with the height of 15 mm and diameter of 10 mm were prepared for Isothermal compression tests, which were carried out on the Gleeble-1500D thermal simulator in the temperature range of 320 - 440 ℃ and the strain rate range of 0.001 - 1 s^{-1}. The height reduction is 60%. Samples were heated with 10 ℃/s, and held for 180 s, and quenched in water for reserving deformed microstructures at the end. The graphite lubricant was set at the end face of samples to minimize the friction between the dies and specimens[4,5,18]. To observe the deformed microstructure, samples were sectioned from the compressed specimens along the compression axis, followed by grinding and mechanical polishing. Samples for electron backscatter diffraction (EBSD) analysis were electropolished in a solution of 90% alcohol and 10% $HClO_4$ at 20-25 V for 5-7 s and observed on a JEOL JSM 7001F scanning electron microscope (SEM), which was equipped for EBSD measurements.

Table 1 The composition of 7056 aluminum alloy

Composition	Zn	Mg	Cu	Zr	Fe	Al
Content/wt%	9.39	1.92	1.98	0.1	0.05	Bal

3 Results and discussion

Flow stress behavior and the constitutive model

The flow stress - true strain curves are shown in Fig.1. In all conditions, the flow stress increases rapidly in a very small strain, showing a greater strain hardening. In this stage, dynamic softening is too weak to inhibit flow stress increase, however, the increase rate of flow stress is gradually decreasing because the dynamic softening is activating and becoming strong at the same time. The DRX is activated and its beginning will change the flow stress behavior. The flow stress reaches a peak when the dynamic softening balances with the strain hardening, and then it keeps constant until the end of tests. Noticeable, the flow stress has

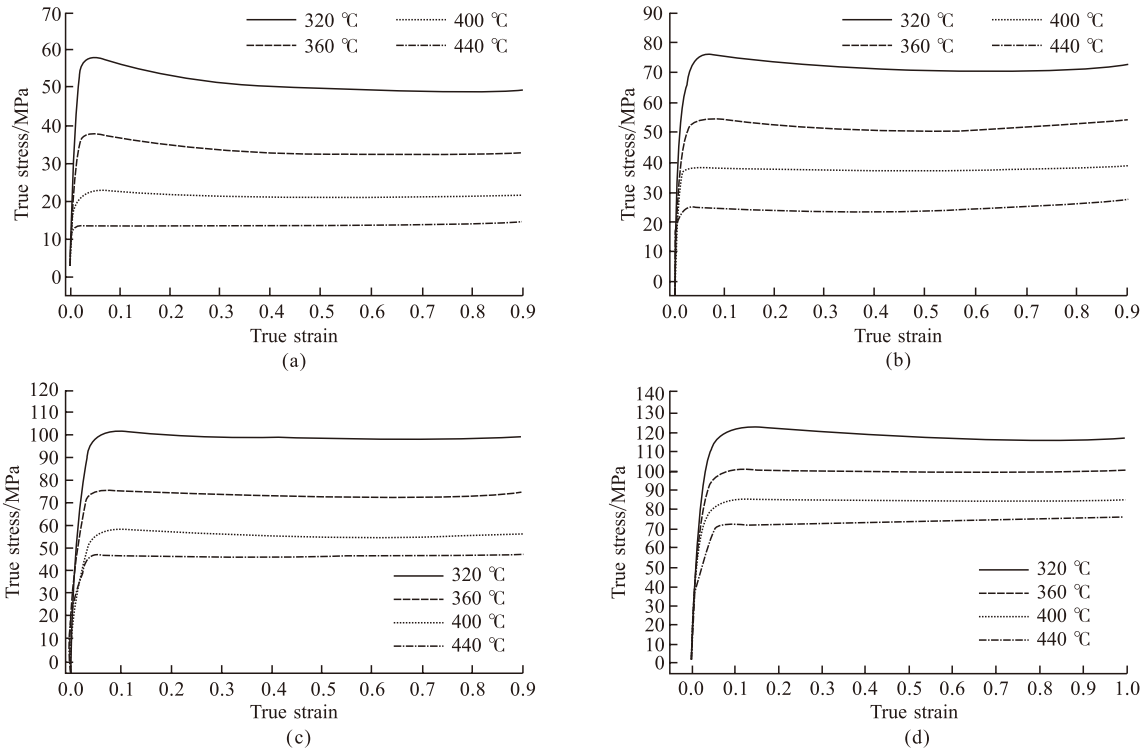

Fig.1 Flow stress curves of 7 056 aluminum alloys: (a) 0.001 s^{-1}; (b) 0.01 s^{-1}; (c) 0.1 s^{-1}; (d) 1 s^{-1}

a slight decrease after peak, especially at the low strain rate and the low temperature. It is a common issue resulting from the $MgZn_2$ particles dynamic precipitating and growing in the deform process. The flow stress is sensitive to the deformation conditions, and it decreases with the deformation temperature increasing and strain rate decreasing as shown in Fig.1.

There are many types of constitutive model for hot deformation processing. Three major categories of these models exist: phenomenological, physical, and artificial neural network (ANN) models[21]. In this study, a classical Arrhenius-type constitutive equation belongs to phenomenological is introduced to describe the flow stress behavior under various deformation conditions[19-21], as follows:

$$\dot{\varepsilon}=Af(\sigma)\exp(-Q/RT) \tag{1}$$

$$f(\sigma)=A_1\sigma^{n_1} \tag{2}$$

$$f(\sigma)=A_2\exp(\beta\sigma) \tag{3}$$

$$f(\sigma)=A[\sinh(\alpha\sigma)]^n \tag{4}$$

where $\dot{\varepsilon}$ is strain rate, Q is activation energy, R is gas constant, T is the absolute temperature, A is structure factor, α is the stress level parameter, n is the stress exponent, A_1, A_2, A, n_1, n, α and β are material constants, in which $\alpha=\beta/n_1$. Substitute $f(\sigma)$ into Eq.(1) and take logarithm, the following equations can be obtained:

$$\ln\dot{\varepsilon}=n_1\ln\sigma+\ln A_1-Q/RT \tag{5}$$

$$\ln\dot{\varepsilon}=\beta\sigma+\ln A_2-Q/RT \tag{6}$$

$$\ln\dot{\varepsilon}=n\ln[\sinh(\alpha\sigma)]+\ln A-Q/RT \tag{7}$$

As shown in Fig.2, according the above equations, $n1$ and β are acquired via calculating the slope of $\ln\varepsilon$-$\ln\sigma$ and $\ln\varepsilon$-σ curves respectively. When the temperature is kept constant, n is calculated from the slope of the $\ln\varepsilon$-$\ln[\sinh(\alpha\sigma)]$ curve, and when the strain rate is kept constant, Q can be obtained from the slope of the $\ln[\sinh(\alpha\sigma)]$-Q/RT curve. The peak flow stresses under various deformation conditions are selected to calculate these parameters, and results are shown as following: n_1=6.568 5, β=0.1047 9, α=0.015 95 MPa^{-1}, n=4.75, Q=140 kJ/mol, $A=5.89\times10^9$. The constitutive equation of 7056 aluminum alloys is shown as follows:

$$\dot{\varepsilon}=5.89\times10^9[\sinh(0.015\ 95\sigma)]^{4.75}\exp(-\frac{140\ 000}{RT}) \tag{8}$$

Critical state of the onset of DRX under various conditions

The critical state of the onset of DRX fixes in the inflection point of Strain hardening rate (θ)-stress (σ) curves obtained by deriving the stress - strain curves, as shown in Fig.3. Black points represent the θ corresponding to each stress. Since the onset of DRX locates in strain hardening stage, only the stresses in the range of 0-σ_p are selected and displayed.

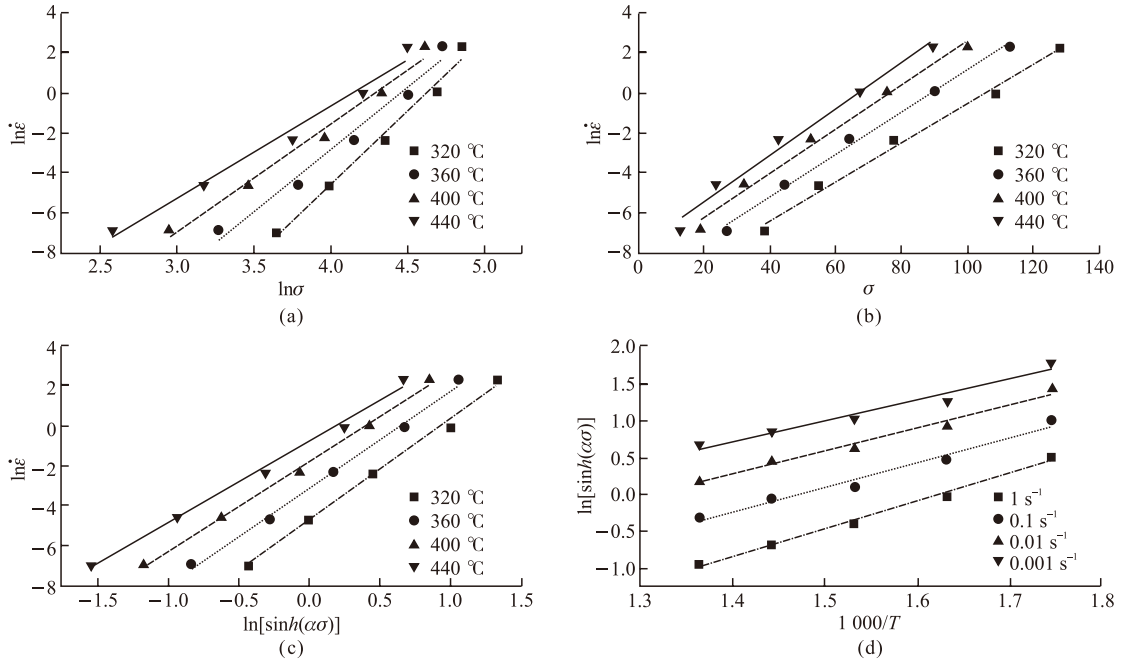

Fig. 2 Relationship between strain rate and flow stress: (a) $\ln\varepsilon-\ln\sigma$; (b) $\ln\varepsilon-\sigma$; (c) $\ln\varepsilon-\ln[\sinh(\alpha\sigma)]$; (d) $\ln[\sinh(\alpha\sigma)]-1\ 000/T$

Table 2 Critical values of 7056 aluminum alloy under different deformation conditions

Temperature /℃	Strain rate/s^{-1}	σ_c/MPa	ε_c	σ_p/MPa	ε_p
320	0.001	48.70	0.019 6	59.18	0.068 1
	0.01	51.30	0.017 4	79.51	0.090 2
	0.1	90.35	0.051 0	106.97	0.227 8
	1	92.25	0.039 3	123.56	0.100 5
360	0.001	21.35	0.010 5	38.29	0.095 2
	0.01	30.80	0.018 4	54.73	0.097 7
	0.1	43.10	0.021 8	75.04	0.099 2
	1	67.70	0.040 9	97.11	0.098 8
400	0.001	18.98	0.017 6	26.30	0.100 1
	0.01	24.50	0.015 2	42.12	0.079 5
	0.1	42.69	0.014 0	63.97	0.077 6
	1	49.98	0.013 2	89.75	0.101 7
440	0.001	14.94	0.006 4	19.10	0.041 8
	0.01	23.44	0.009 4	32.15	0.053 3
	0.1	25.32	0.006 5	52.94	0.066 2
	1	47.83	0.012 2	75.43	0.094 5

According the research of Mirzadeh[22] and Jonas[23], the θ-σ curve is obtained by cubic polynomial fitting, as follows:

$$\theta=A\sigma^3+B\sigma^2+C\sigma \tag{9}$$

where A, B, C and D are functional coefficient constants. Then the second derivative of Eq.(9) with respect to σ can be described as:

$$\frac{d^2\theta}{d\sigma^2}=6A\sigma+2B \tag{10}$$

When the above equation equals zero, the critical stress (σ_c) can be calculated and the corresponding critical strain ε_c can be acquired according to the flow stress curves as shown in Fig.1.

$$\sigma_c=-B/3A \tag{11}$$

The line in Fig.3 is the θ-σ^3 curve for 360 ℃ and 0.1 s^{-1}, which has a high coincidence with the black points. The triangle symbol is the inflection point of this curve, whose corresponding stress is the critical stress of the onset of DRX. Using this method, the critical stress for the other deformation conditions are obtained and shown in Table 2. The corresponding critical strain, peak stress and peak strain are also given. The σ_c and σ_p have a similar law with deformation conditions, they decrease as the temperature increasing and the strain rate decreasing, but there is no monotonous relationship between ε_c, ε_p and deformation conditions.

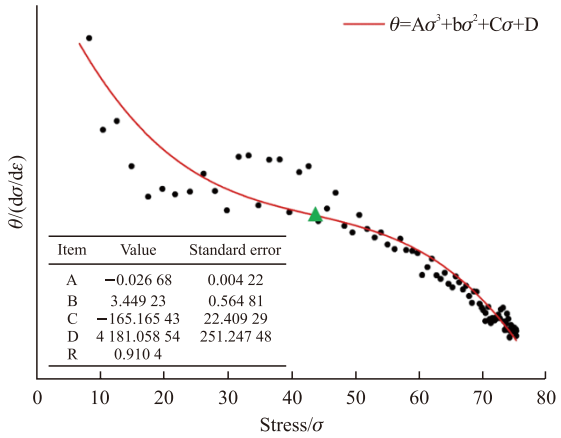

Fig.3 θ-σ^3 curves of the 7056 aluminum alloy at 360 ℃ and 0.1 s^{-1}

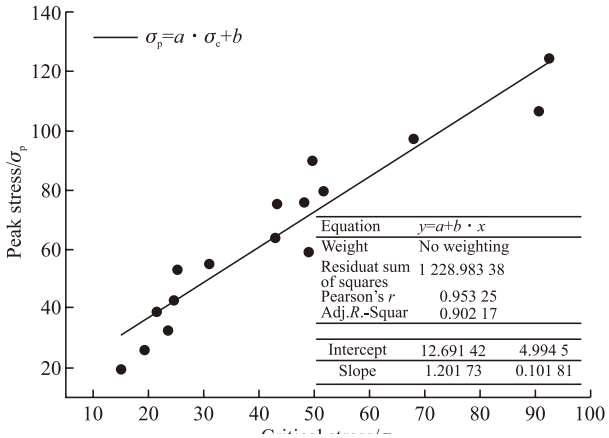

Fig.4 The relationship between critical stress (σ_c) and peak stress (σ_p)

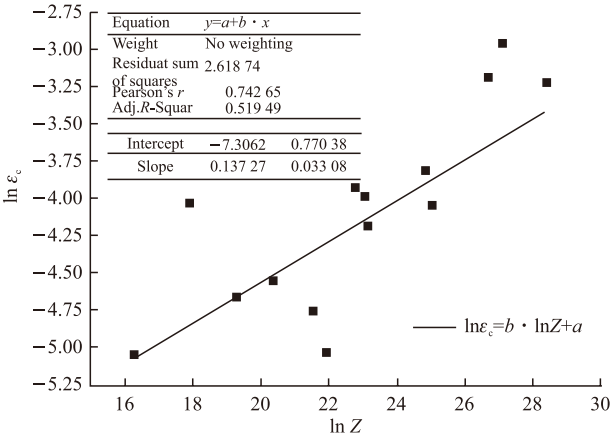

Fig.5 The relationship between critical strain (ε_c) and Z parameter

Fig.4 shows there is a liner functional relationship between σ_c and σ_p, σ_p=1.2σ_c+12.69. Thus, the critical state of σ_c can be acquired by the above equation immediately. In order to build the relationship between deformation conditions and the critical strain ε_c, the Zener-Hollomon parameter is introduced[24], which

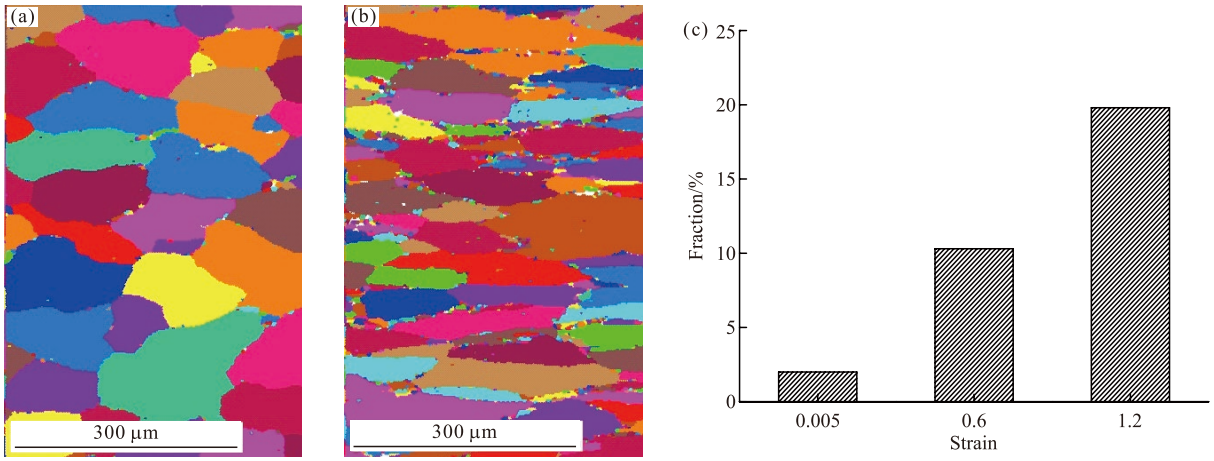

Fig.6 The EBSD microstructure at (a) ε = 0.05 and (b) ε = 0.6; (c) the histogram showing the volume fraction of DRX grains at various strain

takes into account both the temperature and strain rate based on Sellars model[25]. The expression of Z is shown as follows:

$$Z=\dot{\varepsilon}\exp(\frac{Q}{RT}) \tag{12}$$

The critical strains can be expressed as a power-law function:

$$\varepsilon_c=aZ^b \tag{13}$$

Fig.5 shows the relationship between natural logarithm critical strain (ln ε_c) and natural logarithm Zener-Hollomon (ln Z) and the linear fitting result is shown as follows: $\varepsilon_c=6.71\times10^{-4}Z^{0.137\,3}$. Thus, the critical state of ε_c can be acquired from deformation conditions immediately.

Microstructure analysis

Fig.6 shows the microstructure of 7056 aluminum alloys deformed under 360 ℃ and 0.01 s^{-1}. Fig.6(a) gives the microstructure at ε=0.05, and the DRX grains marked by white circles are found at the triangle of grain boundaries. It demonstrates the DRX has occurred in a very small strain, which is close to critical strain ε_c. When the strain increases to 0.6, as shown in Fig.6(b), there are more recrystallized grains distributing in grain boundaries, showing the DRX is intensified as the strain increasing. However, the number of DRV grains increases finitely as the stain increases. Fig.6(c) shows the volume fraction of recrystallized grains, the proportion of recrystallized grains is only 2% at ε=0.05, and it is still small even the strain reaches 0.9, just 20%. For dynamic softening of 7 056 aluminum alloys, the DRV is the main part, and the DRX is the secondary part, even if the DRX is activated earlier.

4 Conclusions

The flow stress of the 7 056 aluminum alloy decreases as the temperature increasing and the strain rate decreasing. An Arrhenius type constitutive equation is established in the range of deformation temperatures from 320 to 440 ℃ and strain rates from 0.001 to 1 s^{-1} and the equation is shown as follows:

$$\dot{\varepsilon}=5.89\times10^{9}[\sin h(0.015\,95\sigma)]^{4.75}\exp(-\frac{RT}{140\,000})$$

The dynamic recrystallization occurs as soon as hot deformation begins under various deformation conditions. Through a theoretical method, the critical state of the onset of DRX is obtained from the inflection point of the θ-σ curves. A liner relationship between critical stress σ_c and peak stress σ_p has been built as follows: $\sigma_p=1.202\sigma_c+12.691$ and the critical strain ε_c has been described by Z parameter as follows: $\varepsilon_c=6.71\times10^{-4}Z^{0.137\,3}$.

The DRX preferentially forms on the triangular grain boundary in the strain hardening stage, and it gradually intensifies as the strain increasing but the increase is limited. The volume fraction of DRX grains is only 20% when the strain is 0.9.

References

[1] Dursun T, Soutis C. Recent Developments in Advanced aircraft Aluminium Alloys[J]. *Mater. Des.*, 2014, 56: 862-871

[2] Heinz A, Haszler A, Keidel C, *et al*. Recent Development in Aluminium Alloys for Aerospace Applications[J]. *Mater. Sci. Eng. A*, 2000, 280(1): 102-107

[3] Ambrogio G, Filice L, Gagliardi F. Formability of Lightweight Alloys by Hot Incremental Sheet Forming[J]. *Mater. Des*., 2012, 34: 501-508

[4] Liu X G, Han S, Chen L, *et al*. Flow Behavior and Microstructural

Evolution of 7A85 High-strength Aluminum Alloy during Hot Deformation[J]. *Metall. Mater. Trans. A*, 2017, 48(5): 2 336-2 348

[5] Shaha S K, Czerwinski F, Kasprzak W, *et al*. Interaction between Nano-precipitates and Dislocations during High Temperature Deformation of Al-Si Alloys[J]. *J. Alloy. Compd.*, 2017(712): 219-224

[6] Shi C J, Lai J, Chen X G. Microstructural Evolution and Dynamic Softening Mechanisms of Al-Zn-Mg-Cu Alloy during Hot Compressive Deformation[J]. *Materials*, 2014, 7(1): 244-264

[7] Mc Queen H J. *Hot Deformation and Processing of Aluminum Alloys* [M]. Boca Raton: CRC Press, 2011

[8] Quey R, Driver J H. Microtexture Tracking of Sub-Boundary Evolution During Hot Deformation of Aluminium[J]. *Mater. Charact*., 2011, 62(12): 1 222-1 227

[9] Son K T, Kim M H, Kim S W, *et al.* Evaluation of Hot Deformation Characteristics in Modified AA5052 using Processing Map and Activation Energy Map under Deformation Heating[J]. *J. Alloy. Compd*., 2018, 740: 96-108

[10] Sun Y, Cao Z H, Wan Z P, *et al.* 3D Processing Map and Hot Deformation Behavior of 6A02 Aluminum Alloy[J]. *J. Alloy. Compd.*, 2018, 742: 356-368

[11] Huang X, Zhang H, Han Y, *et al.* Hot Deformation Behavior of 2026 Aluminum Alloy during Compression at Elevated Temperature[J]. *Mater. Sci. Eng. A*, 2010, 527(3): 485-490

[12] Li J, Shen J, Yan X, *et al.* Microstructure Evolution of 7050 Aluminum Alloy during Hot Deformation[J]. *T. Nonferr. Metal. Soc.*, 2010, 20(2): 189-194

[13] Liu J, Cui Z S, Ruan L Q. A New Kinetics Model of Dynamic Recrystallization for Magnesium Alloy AZ31B[J]. *Mater. Sci. Eng. A*, 2011, 529: 300-310

[14] Quan G, Mao Y, Li G, *et al.* A Characterization for the Dynamic Recrystallization Kinetics of As-extruded 7075 Aluminum Alloy Based on True Stress–strain Curves[J]. *Comp. Mater. Sci.*, 2012, 55: 65-72

[15] Quan G Z, Li G S, Chen T, *et al.* Dynamic Recrystallization Kinetics of 42CrMo Steel during Compression at Different Temperatures and Strain Rates[J]. *Mater. Sci. Eng. A*, 2011, 528(13-14): 4 643-4 651

[16] Wang M H, Li Y F, Wang W, *et al.* Quantitative Analysis of Work Hardening and Dynamic Softening Behavior of Low Carbon Alloy Steel Based on the Flow Stress[J]. *Mater. Des*., 2013(45): 384-392

[17] Chen X, C L Y, Wen D, *et al.* Dynamic Recrystallization Behavior of A Typical Nickel-based Superalloy during Hot Deformation[J]. *Mater. Des*., 2014, 57(5): 568-577

[18] Shi C J, Chen X G. Evolution of Activation Energies for Hot Deformation of 7150 Aluminum Alloys with Various Zr and V Additions[J]. *Mater. Sci. Eng. A*, 2016, 650: 197-209

[19] Huang C Q, Deng J, Wang S X, *et al.* A Physical-based Constitutive Model to Describe the Strain-hardening and Dynamic Recovery Behaviors of 5754 Aluminum Alloy[J]. *Mater. Sci. Eng. A*, 2017, 699: 106-113

[20] Lin Y C, Xia Y, Chen X, *et al.* Constitutive Descriptions for Hot Compressed 2124-t851 Aluminum Alloy over A Wide Range of Temperature and Strain Rate[J]. *Comp. Mater. Sci*., 2010, 50(1): 227-233

[21] Wang Y J, Peng J, Zhong L P, *et al*. Modeling and Application of Constitutive Model Considering the Compensation of Strain during Hot Deformation[J]. *J. Alloy. Compd*., 2016, 681: 455-470

[22] Mirzadeh H, Najafizadeh A. Prediction of the Critical Conditions for Initiation of Dynamic Recrystallization[J]. *Mater. Des*., 2010, 31(3): 1 174-1 179

[23] Jonas J J, Poliak E I. The Critical Strain for Dynamic Recrystallization in Rolling Mills[J]. *Materials Science Forum*, 2003, 426: 57-66

[24] Rokni M R, Zarei-Hanzaki A, Roostaei A A, *et al*. An Investigation into the Hot Deformation Characteristics of 7075 Aluminum Alloy[J]. *Mater. Des.*, 2011, 32(4): 2 339-2 344

[25] Sun Y L, Xie J P, Hao S M, *et al.* Dynamic Recrystallization Model of 30% SiC_p/Al Composite[J]. *J. Alloy. Compd*., 2015, 649: 865-871